2–2 composites based on [011]-poled relaxor-ferroelectric single crystals: from the piezoelectric anisotropy to the hydrostatic response

C. R. Bowen*[a], V. Yu. Topolov[b], D. N. Betts[a], H. A. Kim[a]
[a]Materials Research Centre, Dept. of Mechanical Engineering, University of Bath, BA2 7AY Bath, UK; [b]Dept. of Physics, Southern Federal University, 5 Zorge Street, 344090 Rostov-on-Don, Russia

ABSTRACT

In this paper effect of the orientation of the main crystallographic axes on the piezoelectric anisotropy and hydrostatic parameters of 2–2 parallel-connected single crystal (SC) / auxetic polymer composites is analysed. SCs are chosen among the perovskite-type relaxor-ferroelectric solid solutions of $(1 - x)Pb(Zn_{1/3}Nb_{2/3})O_3–xPbTiO_3$ and $xPb(In_{1/2}Nb_{1/2})O_3–yPb(Mg_{1/3}Nb_{2/3})O_3–(1 - x - y)PbTiO_3$. The SC layers in a composite sample are poled along the perovskite unit-cell [011] direction and characterised by *mm*2 symmetry. The orientation of the main crystallographic axes in the SC layer is observed to strongly influence the effective piezoelectric coefficients d_{3j}^*, g_{3j}^*, squared figured of merit $d_{3j}^* g_{3j}^*$, electromechanical coupling factors k_{3j}^* (j = 1, 2 and 3), and hydrostatic analogs of these parameters of the 2–2 composite. A comparison of values of $d_{3j}^* g_{3j}^*$ was first carried out at $d_{31}^* \neq d_{32}^*$ in a wide range of orientations and volume-fraction. Large values of the effective parameters and inequalities $|d_{33}^* / d_{3f}^*| > 5$ and $|k_{33}^* / k_{3f}^*| > 5$ (f = 1 and 2) are achieved at specific orientations of the main crystallographic axes due to the anisotropy of elastic and piezoelectric properties of the SC component. The use of an auxetic polyethylene with a negative Poisson's ratio leads to a significant increase in the hydrostatic parameters of the 2–2 composite. Particular advantages of the studied composites over the conventional ceramic / polymer composites are taken into account for transducer, hydroacoustic and energy-harvesting applications.

Keywords: 2–2 composite, piezoelectric properties, relaxor-ferroelectric single crystal, auxetic polymer, squared figure of merit, anisotropy factor, hydrostatic parameter

1. INTRODUCTION

Piezo-active composites based on perovskite-type single crystals (SCs) of solid solutions of relaxor-ferroelectrics with high piezoelectric activity show outstanding electromechanical properties[1–3] that enable effective conversion of mechanical energy into electric energy and vice versa. In the last decade the effective electromechanical properties and related parameters have been studied in these materials to determine the optimum applications of the composites in piezoelectric transducer, sensor, hydroacoustic, medical, and energy-harvesting applications. The opportunity here is to further improve the performance by creating composites based on relaxor-ferroelectric SCs with optimum crystallographic orientation. These effects have been studied for SC / polymer composites with 2–2[4–6] and 1–3[7] connectivity patterns (in terms of work[8] by Newnham et al.) and enabled the improvement of hydrostatic parameters by optimising the rotations of the main crystallographic axes of the SC component. The relaxor-ferroelectric SC systems of particular interest as a potential component of advanced composites are domain-engineered samples poled along [011] of the perovskite unit cell. Full sets of electromechanical constants have been measured on the [011]-poled SCs of $(1 - x)Pb(Mg_{1/3}Nb_{2/3})O_3–xPbTiO_3$ (PMN–*x*PT)[9,10], $(1 - x)Pb(Z_{1/3}Nnb_{2/3})O_3–xPbTiO_3$ (PZN–*x*PT)[11,12] and $xPb(In_{1/2}Nb_{1/2})O_3–yPb(Mg_{1/3}Nb_{2/3})O_3–(1 - x - y)PbTiO_3$ (PIN–*x*–*y*)[13] from the *mm*2 symmetry class. In this paper we consider examples of 2–2 composites based on the [011]-poled relaxor-ferroelectric SCs to demonstrate the piezoelectric anisotropy and hydrostatic performance of the composites.

*c.r.bowen@bath.ac.uk; phone +44 (0)1225 383660; fax +44 (0)1225 386928; http://www.bath.ac.uk/mech-eng/people/bowen/index.html

2. MODEL CONCEPTS AND AVERAGING PROCEDURE

2.1 Piezo-active 2–2 composites

It is assumed that the piezo-active 2–2 composite represents a system of parallel-connected SC and the polymer layers form a regular laminar structure (Fig. 1). The main crystallographic axes *X*, *Y*, and *Z* of each single-domain SC layer in the initial state are parallel to the co-ordinate axes OX_j as follows: $X \parallel OX_1$, $Y \parallel OX_2$ and $Z \parallel OX_3$. This means that rotation angles in the initial state obey the conditions $\alpha = 0°$ (inset 1 in Fig. 1), $\beta = 0°$ (inset 2 in Fig. 1) and $\gamma = 0°$ (inset 3 in Fig. 1). Hereafter we consider independent rotations that are described in terms of one of the aforementioned angles, α, β or γ. Such modes of rotation make it possible to maintain a polydomain state in the SC layer. It is assumed that at these rotations, the spontaneous polarisation vectors of domains $\boldsymbol{P}_{s,1}$, $\boldsymbol{P}_{s,2}$ *etc*. in the SC layer (insets 1–3 in Fig. 1) are situated either over or in the (X_1OX_2) plane. Hereby the rotation angles obey inequalities[14] $-\arcsin(1/\sqrt{3}) \le \alpha \le \arcsin(1/\sqrt{3})$, $-45° \le \beta \le 45°$ and $0° \le \gamma \le 360°$. The electromechanical properties of the SC on rotation of its main crystallographic axes are determined in the $(X_1X_2X_3)$ system by taking into account the rotation matrices and tensor ranks of the properties.

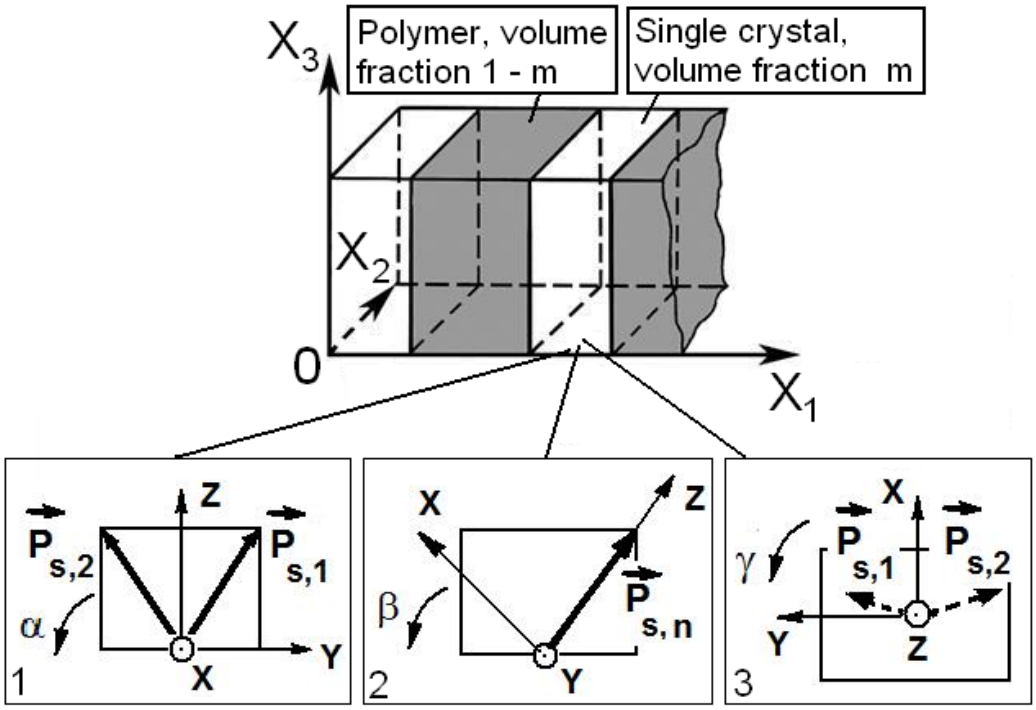

Figure 1. Schematic of the 2–2 SC / polymer composite. $(X_1X_2X_3)$ is the rectangular co-ordinate system of the composite sample. α, β and γ are angles of rotation of the main crystallographic axes *X*, *Y* and *Z* (insets 1–3) in each SC layer. $\boldsymbol{P}_{s1}$, $\boldsymbol{P}_{s2}$, … are spontaneous polarisation vectors of domains in each SC layer.

2.2 Averaging procedure

The effective electromechanical properties of the 2–2 composite are predicted on the basis of the matrix approach[3] that is applied to composites with planar microgeometry. The 9 × 9 matrix of the effective properties of the composite is represented in the rectangular co-ordinate system $(X_1X_2X_3)$ as

$$\| C^* \| = \begin{pmatrix} \| s^{*E} \| & \| d^* \|^t \\ \| d^* \| & \| \varepsilon^{*\sigma} \| \end{pmatrix}, \tag{1}$$

where $\| s^{*E} \|$ is the 6 × 6 matrix of elastic compliances at electric field E = const, $\| d^* \|$ is the 3 × 6 matrix of piezoelectric coefficients, $\| \varepsilon^{*\sigma} \|$ is the 3 × 3 matrix of dielectric permittivities measured at mechanical stress σ = const,

and superscript "*t*" denotes the transposed matrix. The $\| C^* \|$ matrix from Eq. (1) is determined by averaging the electromechanical properties of the components[3] based on the volume fraction *m* and given by

$$\| C^* \| = [\| C^{(1)} \| \cdot \| M \| m + \| C^{(2)} \| (1-m)] \cdot [\| M \| m + \| I \| (1-m)]^{-1}, \quad (2)$$

where $\| C^{(1)} \|$ and $\| C^{(2)} \|$ are matrices of the electromechanical properties of the SC and polymer, respectively, $\| M \|$ is concerned with the electric and mechanical boundary conditions at interfaces $x_1 = \text{const}$ (Fig. 1), $\| I \|$ is the identity 9 × 9 matrix, and $\| C^{(n)} \|$ has a form similar to that shown in Eq. (1). The $\| M \|$ matrix from Eq. (2) is written as $\| M \| = \| m_1 \|^{-1} \| m_2 \|$, where

$$\| m_n \| = \begin{pmatrix} 1 & 0 & 0 & 0 & 0 & 0 & 0 & 0 & 0 \\ s_{12}^{(n),E} & s_{22}^{(n),E} & s_{23}^{(n),E} & s_{24}^{(n),E} & s_{25}^{(n),E} & s_{26}^{(n),E} & d_{12}^{(n)} & d_{22}^{(n)} & d_{32}^{(n)} \\ s_{13}^{(n),E} & s_{23}^{(n),E} & s_{33}^{(n),E} & s_{34}^{(n),E} & s_{35}^{(n),E} & s_{36}^{(n),E} & d_{13}^{(n)} & d_{23}^{(n)} & d_{33}^{(n)} \\ s_{14}^{(n),E} & s_{24}^{(n),E} & s_{34}^{(n),E} & s_{44}^{(n),E} & s_{45}^{(n),E} & s_{46}^{(n),E} & d_{14}^{(n)} & d_{24}^{(n)} & d_{34}^{(n)} \\ 0 & 0 & 0 & 0 & 1 & 0 & 0 & 0 & 0 \\ 0 & 0 & 0 & 0 & 0 & 1 & 0 & 0 & 0 \\ d_{11}^{(n)} & d_{12}^{(n)} & d_{13}^{(n)} & d_{14}^{(n)} & d_{15}^{(n)} & d_{16}^{(n)} & \varepsilon_{11}^{(n),\sigma} & \varepsilon_{12}^{(n),\sigma} & \varepsilon_{13}^{(n),\sigma} \\ 0 & 0 & 0 & 0 & 0 & 0 & 0 & 1 & 0 \\ 0 & 0 & 0 & 0 & 0 & 0 & 0 & 0 & 1 \end{pmatrix}$$

is represented in terms of the electromechanical constants of either SC ($n = 1$) or polymer ($n = 2$) in accordance with the boundary conditions at $x_1 = \text{const}$.

2.3 Effective parameters of the composite

Based on matrix elements of $\| C^* \|$ from Eq. (2) it is possible to determine the volume-fraction (*m*) and orientation (α, β or γ) dependences of effective parameters of the 2–2 composite. Of interest for a variety of applications are

(i) electromechanical coupling factors

$$k_{3j}^* = d_{3j}^* (\varepsilon_{33}^{*\sigma} s_{jj}^{*E})^{-1/2} \quad (3)$$

(j = 1, 2 and 3) and their hydrostatic analog

$$k_h^* = d_h^* (\varepsilon_{33}^{*\sigma} s_h^{*E})^{-1/2}, \quad (4)$$

(ii) anisotropy factors

$$\zeta_{d31} = d_{33}^* / d_{31}^*, \ \zeta_{d32} = d_{33}^* / d_{32}^*, \ \zeta_{k31} = k_{33}^* / k_{31}^* = \zeta_{d31} (s_{11}^{*E} / s_{33}^{*E})^{1/2}, \text{ and } \zeta_{k32} = k_{33}^* / k_{32}^* = \zeta_{d32} (s_{22}^{*E} / s_{33}^{*E})^{1/2}, \quad (5)$$

and (iii) squared figures of merit

$$(Q_{3j}^*)^2 = d_{3j}^* \, g_{3j}^* \quad (6)$$

(j = 1, 2 and 3) and their hydrostatic analog

$$(Q_h^*)^2 = d_h^* \, g_h^* . \quad (7)$$

Electromechanical coupling factors k_{3j}^* and k_h^* from Eqs. (3) and (4), respectively, characterise the effectiveness of the conversion of mechanical energy into electric energy and vice versa. The anisotropy factors from Eqs. (5) enable us

to estimate the possibility of a considerable piezoelectric effect along the OX_3 axis in comparison to the effect along the remaining co-ordinate axes, as well as to find a direction of the preferential conversion of energy in the composite sample. The anisotropy factors from Eqs. (5) are of value for highly-anisotropic piezo-active elements that are used, for instance, in medical diagnostic devices with ultrasonic antennae based on pulse-echo principles and control of the preferred direction, in hydrophones, and other acoustic devices. The squared figures of merit $(Q^*_{3j})^2$ from Eq. (6) are related to power densities, off-resonant energy harvesting[15] and signal-to-noise ratios in piezoelectric transducers[3] and other piezo-technical devices. It should be noted, that contrary to the conventional poled ferroelectric ceramics with $(Q_{33})^2 \neq 0$ (3–3 oscillation mode)[15,16] and $(Q_{31})^2 \neq 0$ (3–1 oscillation mode)[15], we consider three independent oscillation modes [see Eqs. (6)] as a result of the anisotropy of properties of the 2–2 SC / polymer composite (Fig. 1) with interfaces x_1 = const.

The hydrostatic squared figure of merit $(Q^*_h)^2$ from Eq. (7) is important to characterise the signal-to-noise ratios in hydrophones and other hydroacoustic devices. The piezoelectric coefficients d^*_{3j} and g^*_{3j} from Eq. (6) are linked by the relation[17] $d^*_{fp} = \varepsilon^{*\sigma}_{fk}\, g^*_{kp}$ for piezoelectric media. The hydrostatic parameters from Eqs. (4) and (7) characterise the performance of the composite sample (Fig. 1) with electrodes that are parallel to the (X_1OX_2) plane. In this case the hydrostatic piezoelectric coefficients are given by

$$d^*_h = d^*_{33} + d^*_{32} + d^*_{31} \text{ and } g^*_h = g^*_{33} + g^*_{32} + g^*_{31}. \tag{8}$$

The hydrostatic elastic compliance s^{*E}_h from Eq. (4) is represented as $s^{*E}_h = \sum_{a=1}^{3}\sum_{b=1}^{3} s^{*E}_{ab}$, where matrix elements s^{*E}_{ab} are taken from Eqs. (1) and (2).

Electromechanical constants of the SC and polymer components are listed in Table 1. As a comparison, we choose two SC compositions that are very different in terms of the anisotropy of their elastic and piezoelectric properties. Among the polymer components of interest, we choose an auxetic polyethylene (with a Poisson's ratio equal to –0.83)[18]. In recent work[6] this auxetic polymer component was considered in the context of providing anisotropic electromechanical properties in SC / polymer composites. Hereafter we examine the following conditions for a large anisotropy of the piezoelectric coefficients and electromechanical coupling factors of the 2–2 composite:

$$|\zeta_{d31}| \geq 5 \text{ and } |\zeta_{d32}| \geq 5 \tag{9}$$

and

$$|\zeta_{k31}| \geq 5 \text{ and } |\zeta_{k32}| \geq 5. \tag{10}$$

3. RESULTS AND DISCUSSION

3.1. Anisotropy Factors ζ_{d3j} and ζ_{k3j}

When comparing the data on the [011]-poled SCs in Table 1 we observe that the PIN–0.27–0.40 SC exhibits a more pronounced anisotropy of elastic compliances and piezoelectric coefficients compared to PZN–0.07PT. The PIN–0.27–0.40 SC also exhibits larger shear piezoelectric coefficients (e.g. d_{15} and d_{24}) than the longitudinal coefficients (e.g. d_{33}, d_{31} and d_{32}). On examination of the anisotropy factors from Eqs. (5) we observe in Table 2 a wide range of volume-fractions (m) and orientations (γ) wherein conditions (9) and (10) are valid simultaneously.

The strong elastic anisotropy of the PIN–0.27–0.40 SC influences ζ_{k3j} stronger than ζ_{d3j}, and this influence leads to a narrower range of γ (see Table 2). This angle is associated with the rotation of the main crystallographic axes about Z (or the co-ordinate axis OX_3 in Fig. 1), and such a rotation mode strongly influences d^*_{32} and d^*_{31} of the composite. Fig. 2 suggests that conditions $d^*_{31} = 0$ and $d^*_{32} = 0$ are valid when the γ values are close to those listed in Table 2. This means that the large piezoelectric anisotropy of the PIN–0.27–0.40-based 2–2 composite is a result of the orientation effects of the crystallographic axes, the considerable elastic anisotropy of the SC component and the negative Poisson's ratio of the polymer component.

Table 1. Room-temperature elastic compliances s_{ab}^E (in 10^{-12} Pa^{-1}), piezoelectric coefficients d_{ij} (in pC / N) and dielectric permittivities $\varepsilon_{pp}^{\sigma}$ of [011]-poled PZN–0.07PT[12] and PIN–0.27–0.40[13] SCs and auxetic PE[18]

Composition	s_{11}^E	s_{12}^E	s_{13}^E	s_{22}^E	s_{23}^E	s_{33}^E	s_{44}^E
PZN–0.07PT	67.52	–60.16	3.355	102.00	–54.47	62.02	15.45
PIN–0.27–0.40	9.20	–8.38	5.64	21.2	–14.4	16.8	78.1
Auxetic PE	5260	4360	4360	5260	4360	5260	$1.92 \cdot 10^4$
Composition	s_{55}^E	s_{66}^E	d_{15}	d_{24}	d_{31}	d_{32}	d_{33}
PZN–0.07PT	291.55	14.08	1823	50	478	–1460	1150
PIN–0.27–0.40	316	15.5	4550	4100	153	–346	350
Auxetic PE	$1.92 \cdot 10^4$	$1.92 \cdot 10^4$	0	0	0	0	0
Composition	$\frac{\varepsilon_{11}^{\sigma}}{\varepsilon_0}$	$\frac{\varepsilon_{22}^{\sigma}}{\varepsilon_0}$	$\frac{\varepsilon_{33}^{\sigma}}{\varepsilon_0}$				
PZN–0.07PT	8240	1865	3180				
PIN–0.27–0.40	8070	30000	1500				
Auxetic PE	2.3[a]	2.3[a]	2.3[a]				

[a] It is assumed that relative dielectric permittivity equals 2.3, as is known for monolithic PE samples[19]

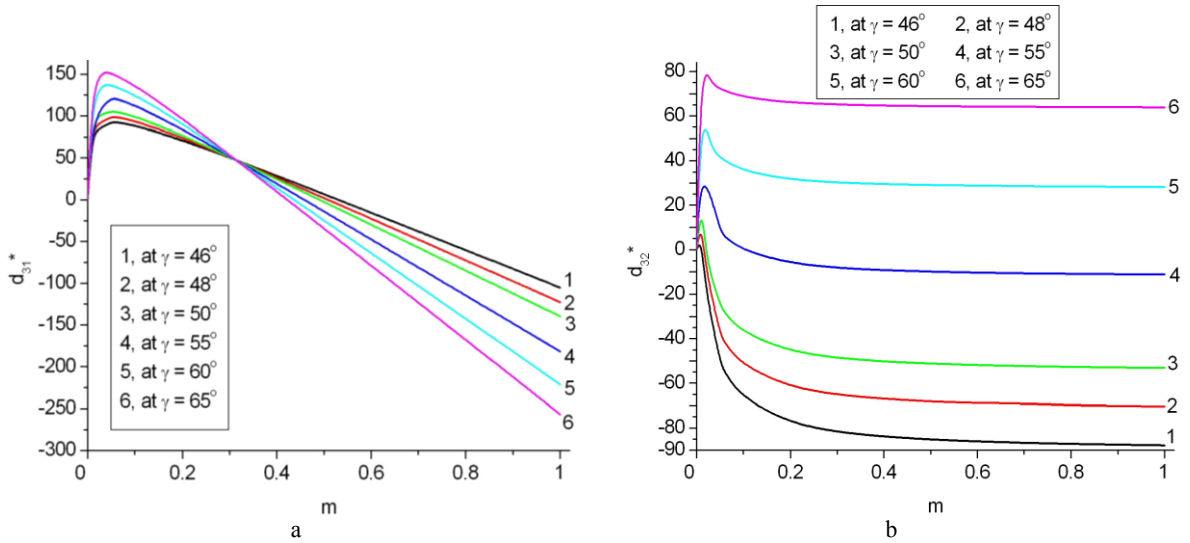

Figure 2. Volume-fraction dependences of piezoelectric coefficients d_{31}^* (a, in pC / N) and d_{32}^* (b, in pC / N) of the PIN–0.27–0.40 SC / auxetic PE composite at γ = const.

3.2. Squared Figures of Merit $(Q_{3j}^*)^2$

The obvious anisotropy of the piezoelectric coefficients d_{3j}^* and, therefore, g_{3j}^* of the 2–2 composite influence its squared figures of merit $(Q_{3j}^*)^2$ from Eqs. (6). To the best of our knowledge, there are no publications devoted to a comparative analysis of $(Q_{3j}^*)^2$ related to different crystallographic directions and/or orientation effects in the SC / polymer composites. The macroscopic *mm*2 symmetry of the [011]-poled SCs[9–13] enables us to compare the piezoelectric response and, therefore, the figures of merit of the composite (Fig. 1) along the different co-ordinate axes OX_j.

Table 2. Volume-fraction ranges [m_1; m_2] wherein conditions (9) and (10) are valid for the 2–2 PIN–0.27–0.40 SC / auxetic PE composite at variations of the rotation angle γ

γ, deg	[m_1; m_2] related to the valid condition (9)	[m_1; m_2] related to the valid condition (10)
47	---	[0.031; 0.037]
48	[0.238; 0.759]	[0.033; 0.049]
49	[0.236; 0.765]	[0.035; 0.070]
50	[0.239; 0.745]	[0,037; 0.124]
51	[0.242; 0.726]	[0.039; 0.484]
52	[0.245; 0.709]	[0.041; 0.950]
53	[0.248; 0.693]	[0.043; 0.945]
54	[0.250; 0.679]	[0.045; 0.940]
55	[0.252; 0.666]	[0.047; 0.936]
56	[0.254; 0.654]	[0.049; 0.929]
57	[0.256; 0.643]	[0.051; 0.924]
58	[0.257; 0.632]	[0.053; 0.919]
59	[0.259; 0.623]	[0.055; 0.913]
60	[0,260; 0.614]	[0.056; 0.908]
61	[0.262; 0.606]	[0.116; 0.903]
62	[0.263; 0.598]	[0.826; 0.898]
63	[0.264; 0.591]	---
64	[0.265; 0.585]	---
65	[0.266; 0.579]	---

A simple comparison of d_{3j}^*, g_{3j}^* and $(Q_{3j}^*)^2$ enables us to observe that the largest values of $(Q_{3j}^*)^2$ are related to $j = 3$ and variations of γ (see inset 3 in Fig. 1): for instance, in the PZN–0.07PT-based composite absolute max[$(Q_{33}^*)^2$] and max g_{33}^* are observed at γ = 90° and $0 < m < 0.01$ (Fig. 3). The small volume fractions m of SC allow the composite to reach high piezoelectric sensitivity (increasing $g_{3j}^*)^3$ due to its small dielectric permittivity $\varepsilon_{33}^{*\sigma}$, i.e., when the inequality $\varepsilon_{33}^{*\sigma} << \varepsilon_{33}^{(1),\sigma}$ holds. However these very small m values make it problematic to manufacture a 2–2 composite with $(Q_{3j}^*)^2 > 10^{-9}$ Pa^{-1} (Fig. 3, a) and $g_{33}^* > 1$ V·m / N. As a compromise between performance and manufacturability we examine in Fig. 4 the performance of the composite at $m = 0.05$ and various angles of rotation. Due to the orientation

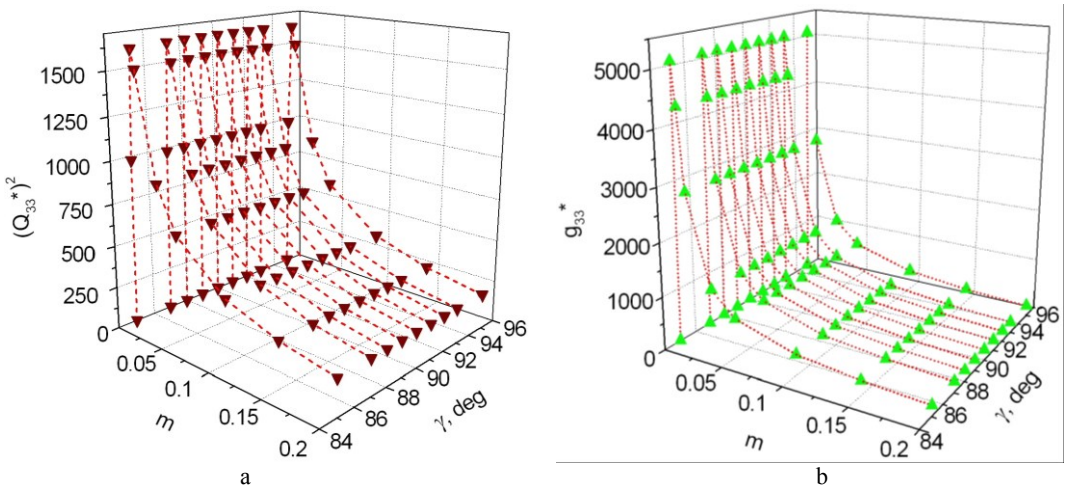

Figure 3. Correlation between the squared figure of merit $[Q_{33}^*(m, \gamma)]^2$ (a, in 10^{-12} Pa^{-1}) and piezoelectric coefficient $g_{3j}^*(m, \gamma)$ (b, in mV·m / N) and of the PZN–0.07PT SC / auxetic PE composite.

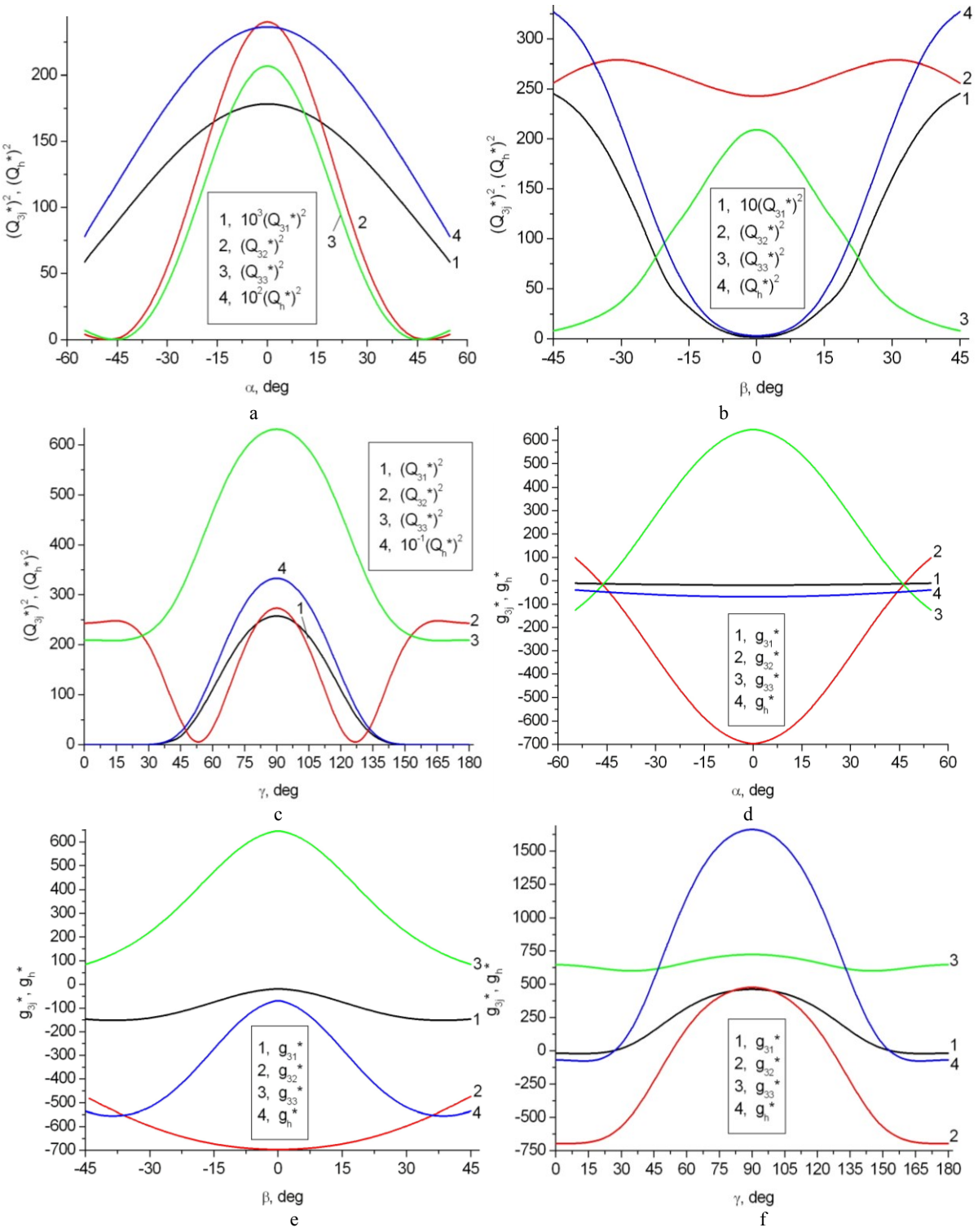

Figure 4. Orientation dependences of squared figures of merit $(Q_{3j}^*)^2$ and $(Q_h^*)^2$ (a–c, in 10^{-12} Pa^{-1}) and piezoelectric coefficients g_{3j}^* and g_h^* (d–f, in mV·m / N) of the PZN–0.07PT SC / auxetic PE composite at m = 0.05.

effect we see a series of extreme points of $(Q^*_{3j})^2$ (see curves 1–3 in Fig. 4, a–c) which correlate with extreme points of g^*_{3j} (see curves 1–3 in Fig. 4, d–f). It is seen that the anisotropy of the squared figures of merit $(Q^*_{3j})^2$ stems from the anisotropy of g^*_{3j} and is varied due to the orientation effect.

3.3. Hydrostatic Parameters d^*_h, g^*_h, $(Q^*_h)^2$, and k^*_h

Data on the hydrostatic parameters of the PZN–0.07PT-based 2-2 composite are shown in Fig. 4 (curves 4) and Fig. 5. We also see the correlation between g^*_h and $(Q^*_h)^2$ at relatively small volume fractions of SC (see curves 4 in Fig. 4). An important observation is the large values of $(Q^*_h)^2$ when varying the rotation angle γ (Fig. 4, c). In Section 3.1 we mentioned the role of the rotation mode (see inset 3 in Fig. 1) in producing a large piezoelectric anisotropy. In this case the inequality

$$(Q^*_h)^2 > (Q^*_{33})^2 \qquad (11)$$

takes place in a wide range of γ (cf. curves 3 and 4 in Fig. 4, c), and $\max(Q^*_h)^2 \approx 3 \cdot 10^{-9}$ Pa^{-1} is very important for hydrophone and related applications. An increase in $(Q^*_h)^2$ is a result of the favourable anisotropy of the piezoelectric coefficients d^*_{3j} from Eqs. (8) and the auxetic polymer component with a negative Poisson ratio that also influences the degree of anisotropy.

It should be added that absolute max d^*_h and max k^*_h are also achieved at γ = 90°. Examination of the hydrostatic parameters near absolute maximum points (Fig. 5) show that a correlation between k^*_h and d^*_h is observed. The large values of k^*_h and d^*_h and volume fractions m at which these values are achieved highlight the advantage of these particular composite structures over the conventional ceramic / polymer composites [3]. The aforementioned correlation may be a result of the strong influence of the piezoelectric properties of the composite on its hydrostatic electromechanical coupling factor from Eq. (4). An additional advantage of the studied composite is also related to the considerable increase in d^*_h (Fig. 5, b) in comparison to $d^{(1)}_h$ of the SC component: according to data from Table 1, $d^{(1)}_h$ = 168 pC / N for the PZN–0.07PT SC.

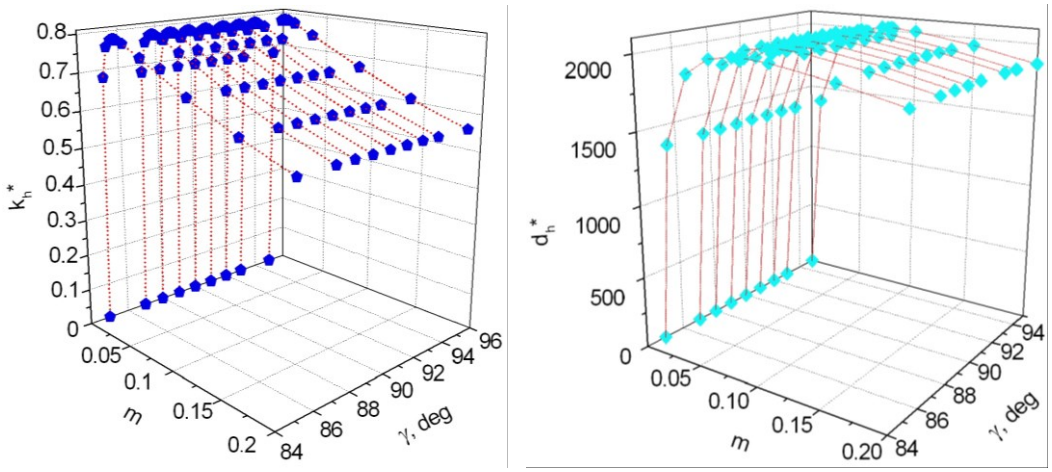

a b

Figure 5. Correlation between the hydrostatic electromechanical coupling factor $k^*_h(m, \gamma)$ (a) and hydrostatic piezoelectric coefficient $d^*_h(m, \gamma)$ (b, in pC / N) of the PZN–0.07PT SC / auxetic PE composite.

4. CONCLUSION

In the present paper we have analysed the performance of the 2–2 composites based on relaxor-ferroelectric SCs poled along [011] of the perovskite unit cell. Various orientations of the main crystallographic axes in the SC layers (see insets 1–3 in Fig. 1) have been analysed to study the polarisation orientation effect on the piezoelectric anisotropy and hydrostatic response of the composites.

Changes in the piezoelectric anisotropy of the SC component due to the polarisation orientation effect influence the anisotropy factors (5) of the composite. An additional influence is caused by the auxetic polymer component with a negative Poisson's ratio that is important for a re-distribution of internal mechanical and electric fields in the composite structure. The anisotropy of the piezoelectric coefficients d_{3j}^* is important for predicting the behaviour of the squared figures of merit $(Q_{3j}^*)^2$ and the hydrostatic piezoelectric response of the studied composites. Conditions (9) and (10) for the large anisotropy of d_{3j}^* and k_{3j}^*, respectively, are valid in the PIN–0.27–0.40 SC-based composite (Table 2). The anisotropy factors obeying conditions (9) and (10), the anisotropy of the squared figures of merit $(Q_{3j}^*)^2$ and correlations between $(Q_{3j}^*)^2$ and g_{3j}^* (Figs. 3 and 4) are important for sensor and energy-harvesting applications. Of particular note for these applications is that in a wide range of composite volume-fractions the values of $(Q_{3j}^*)^2$ (Figs. 3, a and 4, a–c) are larger than $d_{33}.g_{33}$ of conventional poled ferroelectric ceramics[16]. It should be underlined that in the present paper the anisotropy of $(Q_{3j}^*)^2$ has first been discussed for the piezo-active composites based on relaxor-ferroelectric SCs with *mm*2 symmetry. Large values of $(Q_h^*)^2 \approx 3 \cdot 10^{-9}$ Pa^{-1}, $d_h^* \approx 2000$ pC / N and $k_h^* \approx 0.8$ (see curves 4 in Fig. 4 and Fig. 5), as well as validity of condition (11) are of interest for a variety of hydroacoustic applications.

In conclusion, the high performance of the 2–2 SC / polymer composites studied in this paper is highly dependent on the orientation of the main crystallographic axes in the SC layers, and the anisotropy factors, squared figures of merit and hydrostatic parameters of these composites vary at different rotation modes and in wide volume-fraction ranges.

ACKNOWLEDGEMENTS

The authors would like to thank Prof. Dr. R. Stevens (University of Bath, UK), Prof. Dr. P. Bisegna (University of Rome "Tor Vergata", Italy), and Prof. Dr. A. E. Panich and Prof. Dr. I. A. Parinov (Southern Federal University, Russia) for their interest in the performance of advanced piezo-active composites. This work has been carried out with the financial support from the Ministry of Education and Science of Russia within the framework of the Federal Purposive Programme entitled "Studies and Working out on Priority Directions of the Development of the Research Complex of Russia" for 2007–2013, and Prof. Dr. V. Yu. Topolov acknowledges the aforementioned financial support. Prof. Dr. C. R. Bowen would like to acknowledge funding from the European Research Council under the European Union's Seventh Framework Programme (FP/2007-2013) / ERC Grant Agreement no. 320963 on Novel Energy Materials, Engineering Science and Integrated Systems (NEMESIS).

REFERENCES

[1] Ritter, T., Geng, X., Shung, K. K., Lopath, P. D., Park, S.-E., and Shrout, T. R., "Single crystal PZN/PT – polymer composites for ultrasound transducer applications", IEEE Trans. Ultrason. Ferroelec. Freq. Contr. 47, 792–800 (2000).

[2] Ren, K., Liu, Y., Geng, X., Hofmann, H. F., and Zhang, Q. M., "Single crystal PMN–PT / epoxy 1–3 composite for energy-harvesting application", IEEE Trans. Ultrason. Ferroelec. Freq. Contr. 53, 631–638 (2006).

[3] Topolov, V. Yu. and Bowen, C. R., [Electromechanical Properties in Composites Based on Ferroelectrics], Springer, London, 43–99 (2009).

[4] Krivoruchko, A. V. and Topolov, V. Yu., "On the remarkable performance of novel 2–2-type composites based on [011] poled $0.93Pb(Zn_{1/3}Nb_{2/3})O_3 - 0.07PbTiO_3$ single crystals", J. Phys. D: Appl. Phys. 40, 7113–7120 (2007).

[5] Topolov, V. Yu. and Krivoruchko, A. V., "Orientation effects in 2–2 piezocomposites based on $(1 - x)Pb(A_{1/3}Nb_{2/3})O_3–xPbTiO_3$ single crystals (A = Mg or Zn)", J. Appl. Phys. 105, 074105–7 p. (2009).

[6] Topolov, V. Yu., Krivoruchko, A. V., and Bowen, C. R., "Anisotropy of electromechanical properties and hydrostatic response of advanced 2–2-type composites", Phys. Stat. Sol. A 209, 1334–1342 (2012).
[7] Topolov, V. Yu., Krivoruchko, A. V., Bisegna P., and Bowen C. R., "Orientation effects in 1–3 composites based on $0.93Pb(Zn_{1/3}Nb_{2/3})O_3$–$0.07PbTiO_3$ single crystals", Ferroelectrics 376, 140–152 (2008).
[8] Newnham, R. E., Skinner, D. P., and Cross, L. E., "Connectivity and piezoelectric–pyroelectric composites", Mater. Res. Bull. 13, 525–536 (1978).
[9] Liu, G., Jiang, W., Zhu, J., and Cao, W., "Electromechanical properties and anisotropy of single- and multi-domain $0.72Pb(Mg_{1/3}Nb_{2/3})O_3$-$0.28PbTiO_3$ single crystals", Appl. Phys. Lett. 99, 162901 (2011).
[10] Wang, F., Luo, L., Zhou, D., Zhao, X., and Luo, H., "Complete set of elastic, dielectric, and piezoelectric constants of orthorhombic $0.71Pb(Mg_{1/3}Nb_{2/3})O_3$−$0.29PbTiO_3$ single crystal", Appl. Phys. Lett. 90, 212903 (2007).
[11] He, C., Jing, W., Wang, F., Zhu, K., and Qui, J., "Full tensorial elastic, piezoelectric, and dielectric properties characterization of [011]-poled PZN-9%PT single crystal", IEEE Trans. Ultrason. Ferroelec. Freq. Contr. 58, 1127–1130 (2011).
[12] Zhang, R., Jiang, B., Jiang, W., and Cao, W., "Complete set of elastic, dielectric, and piezoelectric coefficients of $0.93Pb(Zn_{1/3}Nb_{2/3})O_3$−$0.07PbTiO_3$ single crystal poled along [011]", Appl. Phys. Lett. 89, 242908 (2006).
[13] Zhang, S., Liu, G., Jiang, W., Luo, J., Cao, W., and Shrout, T. R., "Characterization of single domain $Pb(In_{0.5}Nb_{0.5})O_3$–$Pb(Mg_{1/3}Nb_{2/3})O_3$–$PbTiO_3$ crystals with monoclinic phase", J. Appl. Phys. 110, 064108 (2011).
[14] Topolov, V. Yu., Krivoruchko, A. V., Bowen, C. R., and Panich, A. A., "Hydrostatic piezoelectric coefficients of the 2–2 composite based on [011]-poled $0.71Pb(Mg_{1/3}Nb_{2/3})O_3$–$0.29PbTiO_3$ single crystals", Ferroelectrics 400, 410–416 (2010).
[15] Priya, S., "Criterion for material selection in design of bulk piezoelectric energy harvesters", IEEE Trans. Ultrason. Ferroelec. Freq. Contr. 57, 2610–2612 (2010).
[16] Kim, H., Tadesse, Y., and Priya, S., [Energy Harvesting Technologies], Springer, New York, 3–39 (2009).
[17] Ikeda, T., [Fundamentals of Piezoelectricity], Oxford University Press, Oxford, New York, Toronto, 17 (1990).
[18] Evans, K. E. and Alderson, K. L., "The static and dynamic moduli of auxetic microporous polyethylene", J. Mater. Sci. Lett. 11, 1721–1724 (1992).
[19] [Physics Encyclopaedia], Sovetskaya Entsiklopediya, Moscow, 178 (1983, in Russian).